

# Improving seismic hazard assessment in the Mediterranean region

Rodolfo Console<sup>1,2</sup> and Paola Vannoli<sup>\*,1</sup>

<sup>(1)</sup> Istituto Nazionale di Geofisica e Vulcanologia (INGV), Rome, Italy

<sup>(2)</sup> Center of Integrated Geomorphology for the Mediterranean Area (CGIAM), Potenza, Italy

Article history: received July 27, 2022; accepted November 16, 2022

## Abstract

This paper is intended as a short presentation of the main limitations affecting seismic hazard assessment, revisiting possible methods available in the literature to be applied for this purpose. The convergence of the African Plate with the Eurasian Plate is the cause of the high seismic activity characterizing the Mediterranean region, with particular intensity in its eastern part. It is clear that the associated seismic risk requires appropriate measures for its mitigation. Seismic risk, the amount of resources that the community is expected to pay to earthquakes in the long term, is the product of three factors, such as seismic hazard, vulnerability and value of the exposed goods. As earthquakes cannot be prevented, seismic risk can be mitigated by improving our knowledge of seismic hazard, which is largely based on statistical analysis of historical earthquake catalogs. Nevertheless, historical records are affected by problems of reliability, completeness and shortness, as they commonly span time lengths of the same order of magnitude or even shorter than the inter-event time of the strongest earthquakes produced by specific seismic sources. In this respect, alternative methods can be proposed for integrating and improving our knowledge of seismogenic processes, and estimating both time-independent and time-dependent occurrence rates of strong earthquakes. We propose the application of physics-based earthquake simulators, requiring the knowledge of a robust geological-geophysical seismogenic model.

Keywords: Seismic Hazard Assessment; Statistical analysis; Historical earthquake catalogs; Earthquake simulators; Mediterranean region

---

## 1. Introduction

We know that great earthquakes are likely but rare events in the Mediterranean area, and even earthquakes of relatively low magnitude can cause great damage if the buildings are of low quality or if there are in particularly unfavourable conditions. This may happen especially for communities that have not been affected by strong earthquakes since long time ago [Valensise et al., 2017]. Even earthquakes in the magnitude range 5-6 can be catastrophic, as demonstrated by the 2012 Emilia sequence in Italy ( $M_w$  6.1), which caused casualties and severe damage to monumental and industrial buildings. Therefore, the high rate of seismicity over wide areas of the Mediterranean region produces a high level of earthquake risk, which requires appropriate mitigation measures.

As we describe in Section 3, these measures should aim at optimizing the balance between the costs of protection and the cost of losses due to this particular kind of environmental risk. The approach to the treatment of this thread implies a reliable assessment of earthquake hazard. This contribution to the special issue of *Annals of Geophysics* devoted to environmental hazards in the Mediterranean Basin is intended as a short review of the state of the art and possible progress of seismic hazard assessment in this region.

Earthquake hazard assessment is performed by statistical methods, in terms of probability of exceedance of given earthquake intensities during a given time interval in a specific site (e.g. Rundle et al., 2021 and references therein). This process is largely based on the available information concerning past earthquakes, with important limitations concerning the availability of data reported in the historical records. In the Mediterranean basin we have some of the best historical seismic catalogs in the world [e.g. Guidoboni et al., 1994; Guidoboni and Comastri, 2005] but there are necessary limitations to our knowledge when it comes to going far back in time. In fact, as the average recurrence time between successive large earthquakes of a seismogenic source is generally longer than the period covered by the historical catalogs, there are seismogenic faults for which no large earthquakes are reported, and for most of them only the latest strong event is known [e.g. DISS Working Group, 2021 and reference therein]. These limitations of historical catalogs preclude the application of statistical analysis for seismic hazard assessment, even if it can be partly overcome by geological and paleoseismological investigations on specific faults (see Section 5.1).

In this contribution we conclude that:

- a) it is necessary to support the studies on seismic hazard with geophysical and geological data about earthquake sources, such as the geometrical sizes of active faults and their long-term slip rates, and
- b) the application of recently developed physics-based earthquake simulators could be a useful tool for the improvement of our capacity of understanding and forecasting the seismic processes.

## **2. Seismotectonics of the Mediterranean Area**

The Mediterranean Basin is composed of a complex system of structures generated by the interaction between the Eurasian Plate and the African Plate (Figure 1). This region is the result of a complex geodynamic history: there is still no single comprehensive theory to describe the history of this system, and numerous models have been proposed. According to the Plate Tectonics theory, the two plates have approached with a rotational motion during the last 300 million years, during which the intermediate zones between the two plates were deformed, slipping and rotating against each other, locally either overlapping (thus initiating mountain building) or leaving room for the opening of new internal basins.

The orogenic system that has affected the Mediterranean region forms a very broad and diffuse boundary between the African and European plates that includes intervening microplates (most notably Adria and Anatolia), remnants of closed ocean basins (ophiolites and subduction melanges) as well as still open (Eastern Mediterranean) or newly opened (Western Mediterranean) oceanic domains [see Figure 1; e.g. Schmid et al., 2020; Hasterok et al., 2022].

The process of orogenic formation of the whole Alpine-Himalayan chain was initially driven by the subduction of the Tethyan Ocean beneath Eurasia and has continued even as the ocean has closed in many regions. The continent-continent collisions with Eurasia were heterogeneous in time, beginning with the collision of Apulia (Adria) with Europe ca. 65 Ma [e.g. Hasterok et al., 2022].

The subduction of Ionian oceanic crust underneath the southern margin of the European plate is still active in the Calabrian, Hellenic and Cyprus arcs [Figure 1; see DISS Working Group, 2021 and references therein; <https://diss.ingv.it/diss330/dissmap.html>].

Deep seismicity and tomography data depict a well-developed Calabrian slab down to 500 km depth (Figure 2). The Calabrian subduction zone is characterized by an active back-arc basin in the Tyrrhenian Sea, related to the retreat of the Calabrian slab toward southeast. The Tyrrhenian Sea and a wide Tyrrhenian coastal sector are characterized by thinned crust, very high heat flow [e.g. Della Vedova et al., 2001], and a large number of thermal springs and CO<sub>2</sub> emissions [Vannoli et al., 2021] due to asthenospheric uplift.

In the Hellenic arc, the distribution of the seismicity depicts a well-developed subducting slab beneath the Aegean Sea down to a depth of about 180 km (Figure 2). The Cycladic region and the Aegean Sea as a whole are known to be regions of north-south back-arc extension and thinning continental crust. Nineteen submarine volcanic edifices occur within this small rift zone, the largest of these being Kolumbo which last erupted explosively in 1650 AD, causing significant damage and fatalities on the nearby island of Santorini [e.g. Nomikou et al., 2012].

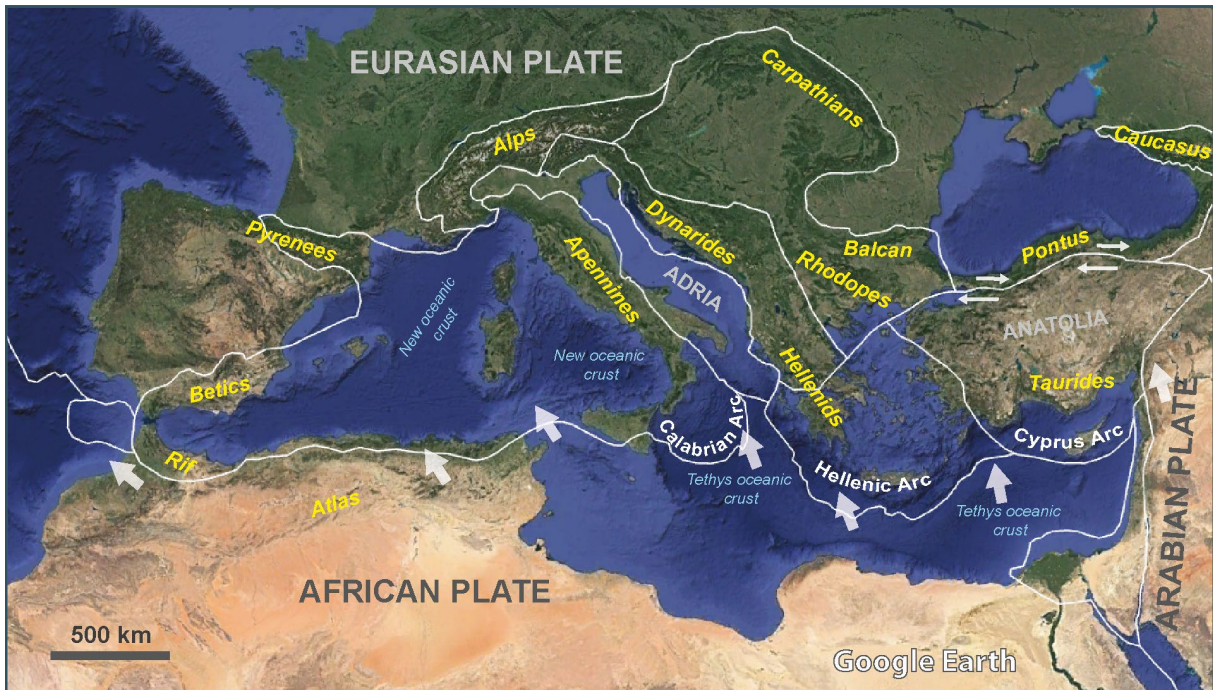


**Figure 1.** Tectonic plate and geologic province model of the Mediterranean area with the three subduction zones of the Calabrian, Hellenic and Cyprus arcs (Hasterok et al., 2022). The main orogens of the Mediterranean region are part of the larger Alpine-Himalayan system and are labeled in yellow. White arrows show the plate motion vectors based on the direction of plate movement (from USGS; <https://www.usgs.gov/media/files/plate-boundaries-kmz-file>).

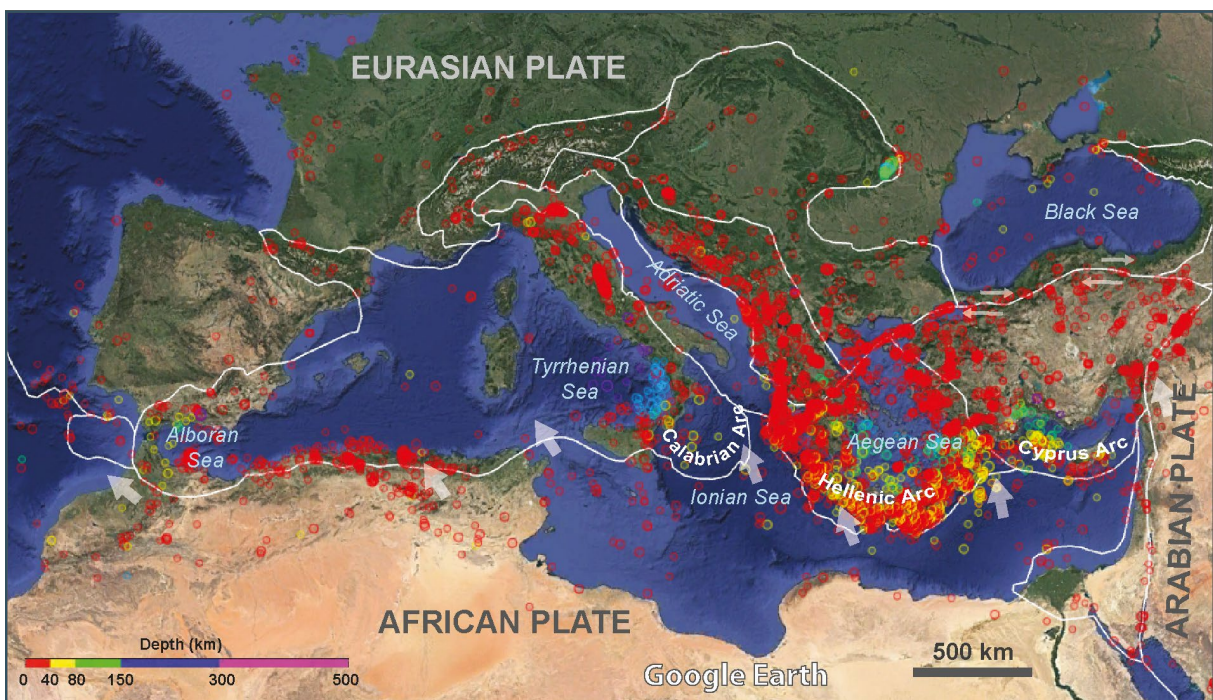


**Figure 2.** Tectonic plate and geologic province model [Hasterok et al., 2022] and earthquakes with a magnitude greater than 4, from 2004 to 2022, in the Mediterranean area. Circle size is relative to the magnitude of the earthquake (data from European-Mediterranean Seismological Centre – EMSC, <https://www.emsc-csem.org>). White arrows show the direction of plate movement (from USGS; <https://www.usgs.gov/media/files/plate-boundaries-kmz-file>).

The Hellenic subduction zone is thought to be capable of generating very large earthquakes and tsunamis. This is mainly testified by the historical, archeological, and geological data available on the 365 AD earthquake and on the effects of its ensuing tsunami [Guidoboni et al., 1994]. In the island of Crete, Pirazzoli and co-authors [1982] estimated a coseismic uplift of 9 meters through the study of the raised and tilted shorelines. Such large coseismic uplift are always associated with very high magnitudes [ $M > 8$ ; e.g. Davies et al., 2018].

East of the Mediterranean, the Cyprus subduction zone is the less known in the region. The seismicity distribution seems to depict a Wadati-Benioff zone beneath the Anatolian microplate down to a depth of about 140 km in the western part of the arc, while in its eastern portion no earthquakes are recorded beyond 60 km depth. In the eastern part of the arc, the subduction zone seems to be evolving towards continental collision, as the crust is not properly oceanic but more probably thinned continental. However, there is no well-defined volcanic arc [DISS Working Group, 2021 and references therein].

In the central Mediterranean region, the Adria microplate played a significant role during the orogenic phases. Interactions between its boundaries and the surrounding continental plates controlled the evolution of the Adria-verging orogenic systems. These plate interactions caused the building of both the Apennine and the Dinaride chains (Figure 1). The present-day structural setting of the Apennines is similar to the other Mediterranean post-collisional thrust-belts, and consists of basement and cover thrust-sheets developed in an ensialic context [e.g. Cosentino et al., 2010]. The geometry of the chain, the diachronism of the eastward migrating foredeep basins, and the different ages of the forethrusts are consistent with a regional foreland propagation model for the Apennines [e.g. Bally et al., 1988].

The Apennines were therefore shaped by contraction at the front of the accretionary wedge overlying the subducting Adria microplate followed by extension at the wedge rear in response to eastward slab rollback. The contraction in the frontal parts of the chains is usually accompanied by extension in the hinterland, with both compressive and extensional fronts migrating towards the foreland with time.

The Mediterranean region can be therefore subdivided into dominantly extensional and dominantly contractional domains. The former can be further split into rifting and mantle upwelling (i.e. along the peri-Tyrrhenian belt), and post-orogenic extension (i.e. along the axis of the Apennines, where the region has undergone continuous regional uplift over the past 1-2 My). The purely contractional domain extends along the frontal portions of the chains (i.e. the Adriatic nearshore and offshore areas).

The Mediterranean basin is also characterized by the presence of the transform boundary between the Eurasian plate and the Anatolian microplate, the North Anatolian Fault. This is an active, ca. 1200-km-long, right-lateral strike-slip system which bounds to the north the Anatolian microplate (Figure 1). This continental transform fault accommodates ca. 20 mm/yr of right-lateral motion, with peak values (up to 300 nanostrain/yr) in the Marmara Sea. In the Mediterranean region, the highest deformation rates are measured, excluding active volcanic areas, in the Gulf of Corinth, with rates up to ca. 400 nanostrain/yr, and along the North Anatolian Fault [Serpelloni et al., 2022].

### 3. Seismic Risk

Seismic risk can be defined quantitatively (from an economic point of view) as the expected cost that the community pays in the long term due to the damage caused by earthquakes, given synthetically by the product:

$$R = S \times V \times Q$$

where

R = risk = cost per time unit (€/year)

S = hazard = frequency of events with intensity exceeding a given level ( $\text{year}^{-1}$ )

V = vulnerability = fraction of value lost by the goods subject to an event of such intensity

Q = total value of the goods exposed to risk (€)

As factor S (seismic hazard) of this product cannot be reduced by any kind of human action, assuming a fixed Q (total value), the only way to reduce R (seismic risk) is acting on factor V (vulnerability). The vulnerability can vary according to the construction criteria adopted for the defense against earthquakes. In principle, the total cost faced

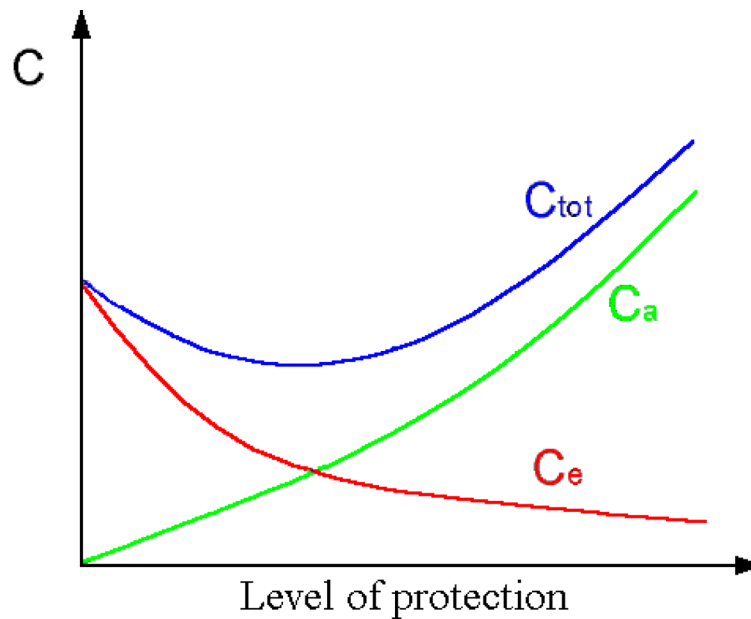


**Figure 3.** Qualitative plot of the costs incurred by the community due to earthquakes as a function of the level of protection adopted:  $C_e$  cost of damages;  $C_a$  cost of prevention measures;  $C_{tot}$  total cost.

by the community living in an earthquake prone region can be divided into two parts, as shown in a qualitative way by Figure 3: the cost of the protection measures that is incurred before the events (for example, adopting stronger criteria in the design of buildings), and the cost that is incurred for the repair of the damage produced by high intensity events. The trends in these costs as a function of the severity of the prevention measures are generally in the opposite direction, respectively decreasing for that of damage, and increasing for that of prevention measures. The curve of the total costs that the community will pay for the earthquake in the long term, typically has a minimum point, which defines the optimal economic criterion for mitigating the risk due to earthquakes. A strategy that adopted a level of protection below the minimum point of the total cost curve (such as ignoring the problem) would not only be criminal towards the safety of people, but also uneconomic. On the contrary, the adoption of a higher level of protection, at the expense of a cost greater than the minimum, would ensure greater safety for the population. How much it would be appropriate to raise the level of protection thus becomes a problem to be solved at a decision-making-political level, in which the necessary balance between the resources that must be distributed among all the possible causes of risk must also be taken into account.

#### 4. The validity of seismic hazard estimates

As we saw in the previous section, the knowledge of the destructive characteristics of earthquakes, and their probability of occurrence in certain time intervals, is a fundamental component of the knowledge that leads to the assessment of seismic risk and its effective mitigation. Italy, like all countries in the world with high seismicity and economically developed, has a specific legislation for constructions in seismic areas, which includes a map of seismic hazard of the national territory [Figure 4; Stucchi et al., 2004]. An update of the Italian seismic hazard map has been recently proposed, even if has not yet formally adopted by the Italian Government [Meletti et al., 2021]. The new model is based on the catalog of strong earthquakes occurring on the national territory [CPTI15; Rovida et al., 2022], and in limited way on the updated information of seismogenic sources recognized as capable of generating earthquakes of magnitude equal to or greater than 5.5 in Italy [DISS Working Group, 2021].

The questions we can ask ourselves are:

- 1) Is it possible to evaluate the validity of the seismic hazard models adopted for the prevention measures, based on the observations?
- 2) Is the model adopted by current legislation the optimal one to minimize damage to people and property caused by earthquakes?

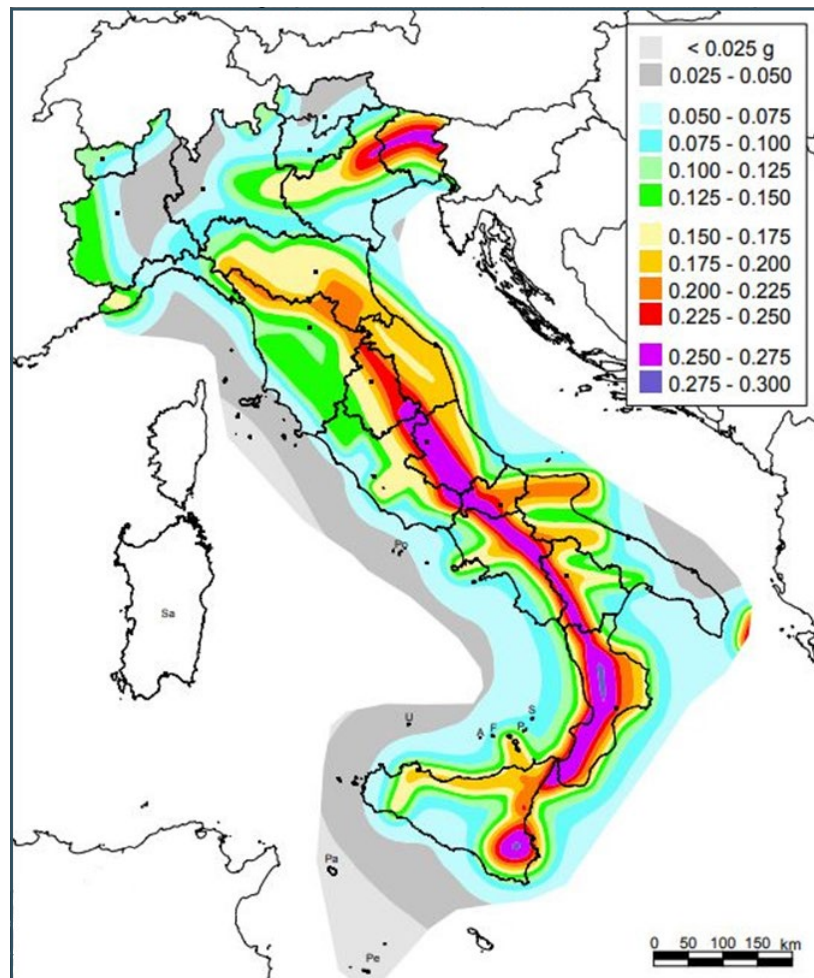


**Figure 4.** Seismic hazard map of the Italian national territory expressed in terms of maximum ground acceleration with 10% probability of exceedance in 50 years [after Stucchi et al., 2004].

It is obvious that a negative answer to the first question precludes the possibility of answering the second.

Some considerations that may help to answer the first question may derive from the analysis of figure 5, which shows the annual frequency of earthquakes occurred in the Central Apennines as a function of their threshold magnitude for three different time intervals, within which the CPTI catalog can be considered complete. In figure 5 the red symbols refer to the catalog starting from 1950, the year from which it is estimated that all earthquakes with a magnitude of at least 4 have been detected. The green and blue symbols represent the data with threshold magnitudes equal to 5 and 6, respectively complete from the year 1871 and 1530. Figure 5 shows that the trend of the accruals, on a logarithmic scale, follows an approximately straight decreasing trend, according to which the number of earthquakes of a given magnitude is roughly one-tenth of those of a magnitude less than one unit (the rule well known as Gutenberg and Richter law). Assuming this law as valid, it would be possible to estimate for any seismic zone the expected frequency of earthquakes of any magnitude as large as desired, simply by extrapolating the trend of the diagram in Figure 5, even if such earthquakes have not yet been actually observed. This possibility would allow to estimate the seismic hazard of an area, simply based on modern and reliable instrumental data.

In reality, there is no certainty as to what are the maximum magnitude values up to which the Gutenberg-Richter law can be assumed to be valid. From Figure 5 it is also very clear that the statistical uncertainty on the obtained values of the occurrence rates, represented by the height of the vertical bars associated with each symbol, grows with the increase of the magnitudes considered. In fact, as established by Poisson's theory of errors, this uncertainty increases as the number of events considered in the analysis decreases.

Figure 5 also shows, with black symbols, the rates obtained for the same seismic zone in Central Italy, by a simulation algorithm based on deterministic physical laws [Console et al., 2018]. This type of algorithm is based on discretized geometrical models of earthquake sources and heuristic rules of nucleation and stopping of earthquake

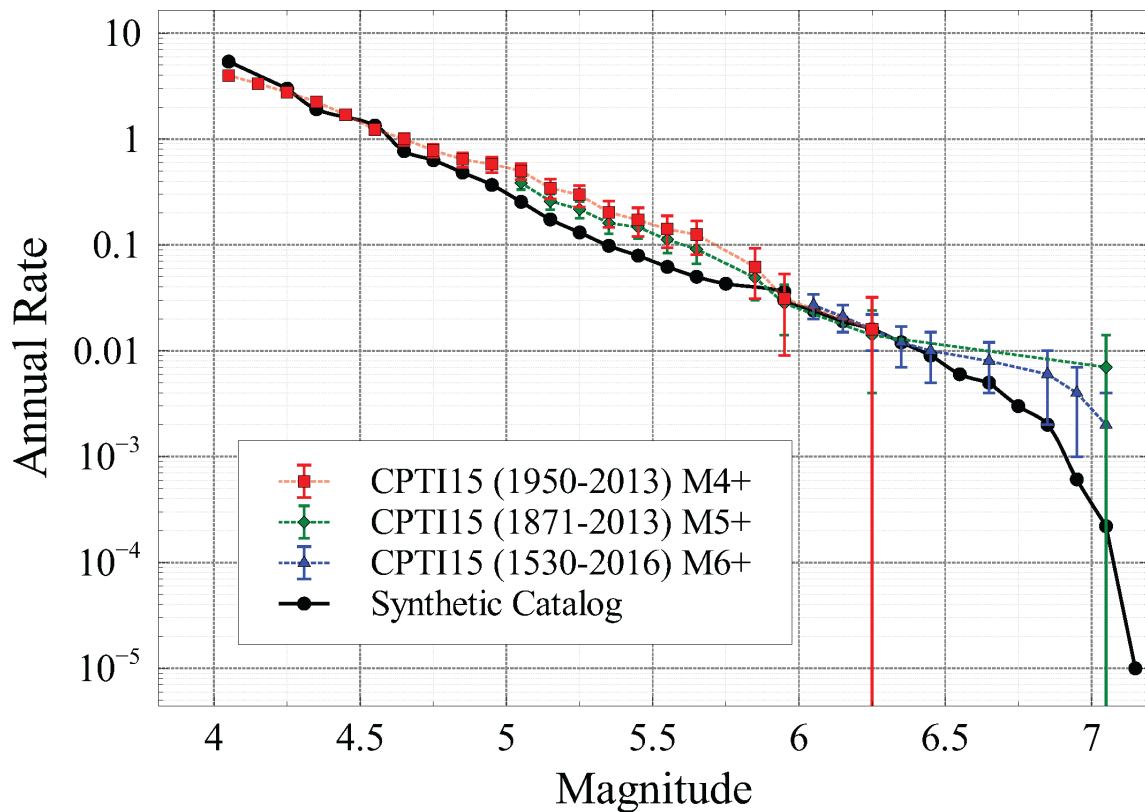


**Figure 5.** Cumulative distribution of the annual rate of earthquakes as a function of magnitude, obtained from a synthetic catalog of 100,000 years for the Central Apennines (black dots), compared with those obtained from the Parametric Catalog of Italian Earthquakes (CPTI15) in the same area for three different time intervals (red, green and blue symbols), within which the catalog itself can be considered complete. The vertical bars indicate the statistical uncertainty of the occurrence rate values obtained from historical and / or instrumental observations [after Console et al., 2018].

ruptures. It can generate, in a few hours of calculation on a computer with good performance, a synthetic catalog lasting 100,000 years, containing over 300,000 earthquakes with a magnitude greater than 4. The comparison between the trend obtained from the simulator and the one from the real catalog, it shows a close analogy in respect of the Gutenberg-Richter law, but also some discrepancies, as in the magnitude interval between 5 and 6, in which the simulator shows a seismic activity lower than that observed.

The most important discrepancy concerns, however, the trend of the curves at the largest magnitudes (higher than 6.5) which are the most relevant for the purposes of seismic hazard estimates. As has already been said, for such large magnitudes the real catalog is based on a very limited number of observed events (even of only one, as in the case of the Avezano earthquake of 1915 of magnitude 7.1, shown in figure 5) and presents very significant uncertainties. For magnitudes greater than 6.5, the black curve, which represents the computer-simulated catalog rates, shows a tendency to decrease faster and faster than the observed data. This depends on the fact that the fault model provided with the input data to the simulation algorithm places physical limits on the energy (and therefore on the magnitude) released by the fracture phenomenon that generates earthquakes: a clear reason that explains the existence of an upper limit of magnitude beyond which the Gutenberg-Richter law cannot be applied.

## 5. Long-term time dependent hazard models

### 5.1 Renewal models

Seismic codes adopted by developed countries are generally based on a time-independent occurrence probability of earthquakes, modelled by the Poisson hypothesis. However, it is commonly observed that the earthquake

occurrence rate in limited areas is strongly variable in time, both in the short- (earthquake clustering) as in the long-term (pseudo-periodicity).

Long-term pseudo-periodicity of strong earthquakes is a simple consequence of the Reid [1910] elastic rebound theory. A more recent expression of this theory can be recognized in the characteristic earthquake model [Schwartz and Coppersmith, 1984; Wesnousky, 1994]. According to this model, belonging to the category of renewal models, strong earthquakes have a general inclination to repeat themselves along the same fault segment or plate boundary. The occurrence of a characteristic earthquake ruptures the entire segment and relieves tectonic stress within the segment. Therefore, the regularity of the inter-event time is just a simple physical consequence. According to this hypothesis, the earthquake hazard is small immediately following the previous large earthquake and increases with time since the latest event on a certain fault or plate boundary. Hence, the earthquake occurrence can be regarded as a quasi-periodic process [McCann et al., 1979; Shimazaki and Nakata, 1980; Nishenko and Buland, 1987].

Console et al. (2002) carried out a statistical comparison of the characteristic earthquake model with respect to the plain memory-less Poisson model, using data extracted by the *Database of earthquake recurrence data from paleoseismology* [Pantosti, 2000], limiting the analysis to four trenches sites in the Mediterranean region (Figure 6) for which at least two inter-event times were available from paleoseismological data. For their test they considered the parameter  $C_v$  (also named aperiodicity), defined as the ratio between the standard deviation  $\sigma$  and the mean inter-event time  $Tr$  of the observed inter-event times. This parameter is equal to 1 for a uniform random distribution.  $C_v < 1$  denotes a periodical occurrence of events and  $C_v > 1$  characterizes clustering of events. To take into account the uncertainties of the observed inter-event times, they used a Monte Carlo procedure, obtaining the following values:

- $C_v = 0.368 \pm 0.148$  for the Irpinia fault,
- $C_v = 0.187 \pm 0.017$  for the Fucino fault,
- $C_v = 0.806 \pm 0.102$  for the El Asnam fault,
- $C_v = 0.656 \pm 0.214$  for the Skinos fault.

Even if these values, especially that of the Fucino fault, appear substantially smaller than 1, they are biased by the small number of inter-event times used in the test. So, by proceeding with the test in a rigorous and quantitative way, Console et al. [2002] concluded that the null hypothesis of the Poisson inter-event distribution can be rejected with a confidence level of 99.5% for the Fucino fault, but it can be rejected only with a confidence level between 90% and 95% for the Irpinia fault, while it can not be rejected for the other two cases.



**Figure 6.** Location of the four faults for which a seismic history was built on the basis of paleoseismological data extracted from the *Database of earthquake recurrence data from paleoseismology* [after Console et al., 2002].



## 5.2 Effect of stress-interaction among faults

Taking a further step towards the physical modeling of the seismogenic process, statistical models were built that take into account the elastic interaction between faults. These models require the calculation of the actual stress change (Coulomb stress change) produced by a seismic dislocation of a given fault on the probable fracture plane of another fault. Using suitable algorithms, this stress variation (positive in the sense that it brings a fault closer to the fracture condition, negative in the sense of moving it away from this condition) is respectively translated into an advance or a delay of the next seismic event with respect to what is expected in conditions unperturbed.

Console et al. [2007, 2010] applied a model of this type to the *Database of the Individual Seismogenic Sources* (version 3.0.2; 2006; <https://diss.ingv.it/data>) for the area of the central-southern Italy. Taking into account the possible interaction of the faults with each other, in addition to the time elapsed since the last earthquake occurred on each single fault, it is possible to calculate the expected rate of an earthquake of the same type at the present time (hazard rate), and from the latter, the conditional probability of having such an earthquake in a given future time period.

Table 1 shows some results obtained from the analysis conducted through this modeling on the two seismogenic sources of the central-southern Apennines shown in Figures 7a and 7b.

Taking into consideration the Sulmona fault (figure 7a), it can be seen that the Avezzano earthquake of 1915 induced a negative Coulomb stress on it, which tends to lighten the value accumulated by deformations of tectonic origin. On the contrary, the earthquakes that occurred on the transcurrent faults located east of Sulmona provide a positive contribution, i.e. they tend to accelerate the tectonic loading process, and therefore to bring the moment of the fracture closer.

The result, shown in Table 1 (first column of values), compares the probability of occurrence of the next characteristic earthquake for the next 50 years, estimated on the basis of different hypotheses. For the model called “Poissonian”, based only on the time of recurrence, and completely independent of time, the maximum probability of a new event in the next fifty years is 5.3%. Taking into account that the time passed since the last earthquake that completely broke the Sulmona fault, that of 3 December 1315, is 692 years, based on a renewal model, with memory, this probability increases to 8.4%. But if we also consider the fact that a possible future event may be favored by a variation in effort determined by what happened in the surrounding areas after 1315, this probability rises further to 11.8%. It must be noted that the most recent version of the DISS Database (<https://diss.ingv.it/>) re-examines and excludes the attribution of the 3 December 1315 earthquake to the Sulmona fault. If the latest large event had occurred earlier, the current probability of occurrence obtained by the renewal model would be significantly higher.

	Sulmona basin	Melandro-Pergola
Date of latest event	1315.12.3	1857.12.16
Slip rate (mm)	$0.24 \pm 0.06$	$0.11 \pm 0.04$
Recurrence time (years)	$2300 \pm 1370$	$4300 \pm 3700$
Max. Poisson probability for the next 50 years	5.3%	8.8%
Elapsed time (years)	692	150
Max. renewal probability for the next 50 years	8.4%	1.8%
Max. $\Delta CFF$ (Mpa)	0.15	0.19
Max. $\Delta t$ (years)	132	394
Max. modified probability for the next 50 years	11.8%	18.6%

**Table 1.** Results of the elastic interaction analysis for two seismogenic sources of the central-southern Apennines [after Console et al., 2007, 2010].

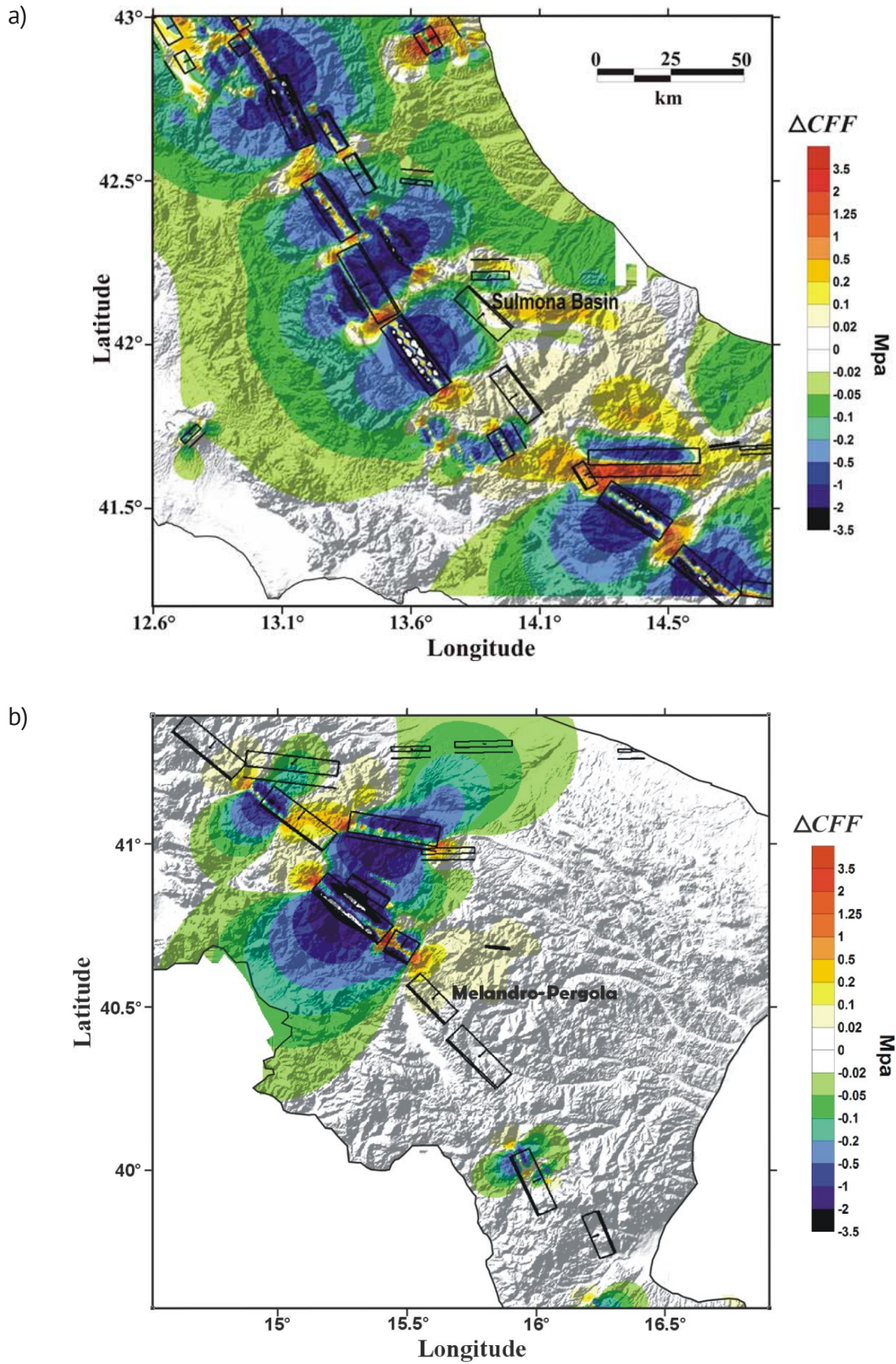


**Figure 7.** Maps of the stress variation caused by seismic events on the sources of the DISS catalog version 3.0.2 (2006) following (a) the Sulmona earthquake of 3 December 1315, and (b) the Val d’Agri earthquake of 16 December 1857. The changes are calculated by assuming on each point of the map an expected mechanism of any induced earthquake equal to that of the past events respectively considered in (a) and (b) [after Console et al., 2008, 2010].

Going a little further south and taking into consideration the Melandro-Pergola fault, one of the two that gave rise to the Val d'Agri earthquake of 16 December 1857, we can see in figure 7b that the Irpinia earthquake of November 1980, for which three sources have been identified that ruptured at a distance of only 20 seconds from each other, had a positive influence, that is, it tends to accelerate the next event on this fault. So, it is as if the seismogenic process had accelerated or, as they usually say, as if the earthquake clock had been put forward again.

Therefore, in this second case, as shown by the second column of the values of Table 1, the maximum Poissonian probability (uniform over time) for the next 50 years is equal to 8.8%. In fact, the minimum recurrence time (average value minus the uncertainty limit) assumed for the Melandro-Pergola fault (600 years) is less than that of the Sulmona fault (930 years). However, for the Melandro-Pergola fault (Val d'Agri) the last characteristic earthquake occurred, so to speak, only 150 years ago. This means that the conditional probability provided by the renewal model drops to just 1.8% for the next 50 years. Finally, including in the calculations the potential effect of the 1980 Irpinia earthquake which, as mentioned, is positive, the conditional probability rises again to 18.6%.

### 5.3 Simulation by a physics-based earthquake simulator

As shown in Figure 5 of Section 4, here in the following we quote a recent case study to show the way by which the application of an earthquake simulator algorithm can provide robust information on the seismogenic process, in comparison with that inferred from a catalog of real observations of limited duration.

Console et al. [2022] applied a physics-based earthquake simulation algorithm to the seismicity of the Corinth Gulf fault system, obtaining a catalog spanning 100,000 years and containing more than 360,000  $M \geq 4.2$  events with a maximum likelihood b-value equal to 1.07. The spatio-temporal pattern of large earthquakes exhibits features that are comparable with the observations. More than 40% of the  $M \geq 6.0$  earthquakes in the simulated catalog are caused by the simultaneous ruptures of significant parts of more than one segment, which appears to be a relevant fraction. In extreme cases, strong earthquakes rupturing five segments simultaneously are noted six times in the 100 kyr simulation period. Typically, these events ruptured adjacent segments for a total length of 80-85 km, releasing a seismic moment of  $1.3\text{-}2.3 \times 10^{19}$  Nm, equivalent to a 6.7-6.8 magnitude earthquake, which seems realistic for the study area. This supports the hypothesis that multi-segmented ruptures are necessary ingredients for the simulator to produce events of magnitude consistent with the largest historical magnitudes ( $M \geq 6.4$ ).

Figure 8 shows the annual cumulative Frequency-Magnitude Distribution (FMD) of the earthquakes in the 100 kyr simulated catalog compared with the instrumental earthquake catalog compiled by the Geophysics Department of the Aristotle University of Thessaloniki (GD-AUTH, <https://doi.org/10.7914/SN/HT>) for the period January 1965 – September 2020. The rate of earthquakes with  $M \geq 4.2$  in the simulated catalog is 3.67/yr, while the corresponding rate of observed earthquakes with  $M \geq 4.2$  in the observed instrumental catalog is 2.98/yr.

The duration of 55 years of this instrumental catalog, shorter than the typical inter-event time for  $M \geq 6.0$  earthquakes on single fault-segments, appears quite short for representing the long-term behavior of this fault system. Thus, the comparisons between the long-term features must be retained as quite questionable.

Figure 8 further shows that the FMD of the simulated catalog does not follow a straight line as expected according to the Gutenberg-Richter law, but exhibits a change in its slope from smaller than 1.0 to larger than 1.0 around magnitude 4.9. This case could be justified by the fact that the source model adopted in our simulation does not include the numerous small sources, capable of producing only small and moderate magnitude events, which coexist in the brittle part of the crust along with the major sources.

Console et al. [2022] compared the changes in seismicity rates observed in their simulated catalog with those ascribed to the phenomenon of accelerated moment release (AMR), frequently observed for years to tens of years before, and over tens to hundreds of kilometers from the epicenter of the anticipated main shock.

The simulated catalog of 100,000 yrs was analyzed by a stacking technique, counting the total number of events with  $M \geq 4.2$  that preceded or followed any other event of  $M \geq 6.0$  in a time window of  $\pm 100$  yrs, in bins of 1 yr, and within a radius of 20 km. The result of this analysis is shown in Figure 9, where an acceleration of seismic rate starting about 40 yrs before the occurrence time of any  $M \geq 6.0$  earthquake is clearly depicted. Figure 9 also shows that quiescence follows the aftershock decay and takes 40-60% of the seismic cycle. Activity is then observed to build up, to a more or less steady background rate, during the latter part of the cycle. A simple explanation for this behaviour is that the regional quiescence that follows the aftershocks results from the region being within the stress

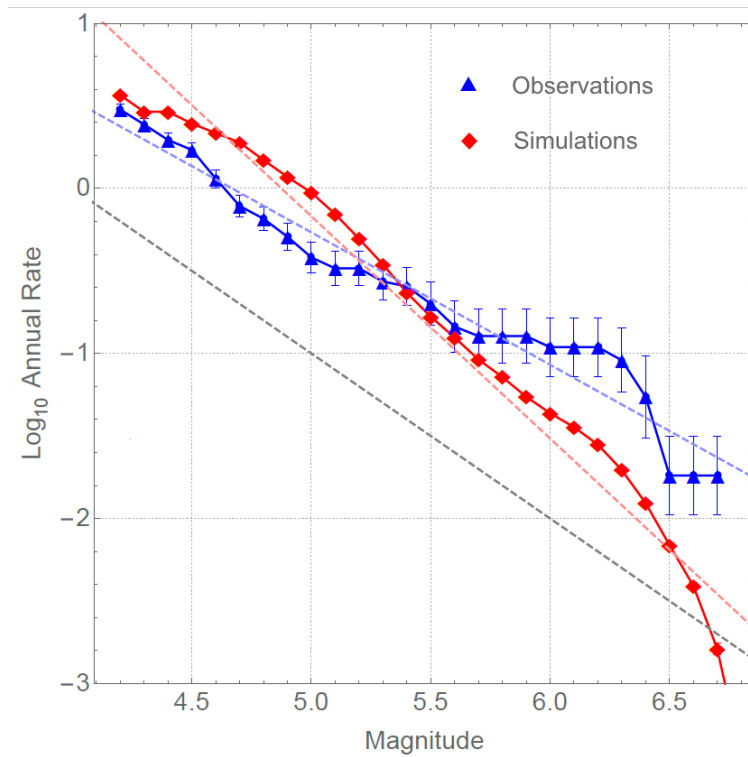


**Figure 8.** Cumulative frequency – magnitude distribution of the earthquakes ( $M \geq 4.2$ ) in the 100,000 yrs simulated catalog (red diamonds) compared with observations, i.e. the events (1965-2020) whose hypocenters are within 10 km from the fault planes (blue triangles). Error bars are provided for the observation. The straight red and blue dashed lines represent their linear regression, respectively. The grey dashed line shows the slope of  $b=1$  for reference [after Console et al., 2022].

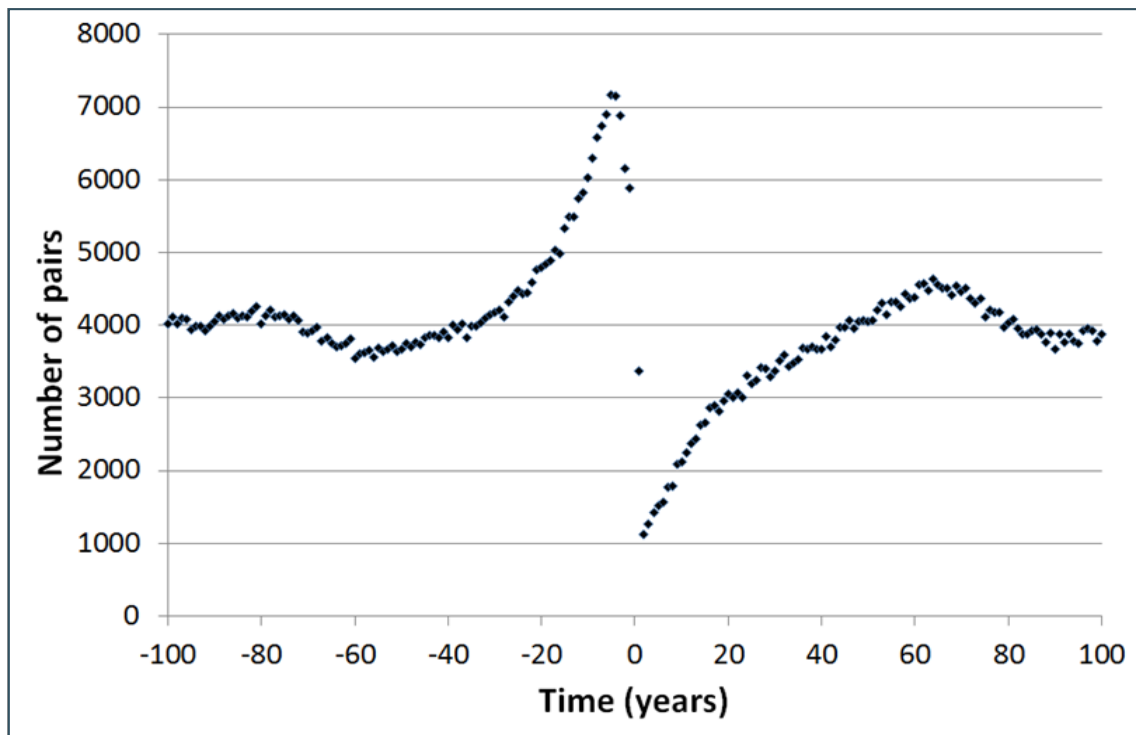


**Figure 9.** Stacked number of  $M \geq 4.2$  events in the 100 yrs period in bins of 1 yr before and after an  $M \geq 6.0$  mainshock and within a radius of 20 km, in the 100,000 yrs simulated catalog of the CGFS [after Console et al., 2022].

shadow of the mainshock. The slip is highly variable within an earthquake rupture, and the fault can be considered to be composed of elements that are heterogeneous at all scales coupled by long- and short-range elastic forces.

## 6. Conclusions

In this short, and necessarily incomplete review on seismic hazard, we have seen that the Mediterranean area is subject in many parts to seismic activity of considerable intensity, which requires adequate prevention measures to ensure reasonable mitigation.

In the absence of any possibility of formulating deterministic forecasts of earthquakes, statistical methods are used, which provide hazard estimates in terms of the probability of exceeding certain values of the effects of earthquakes. After all, even weather forecasts, despite being largely based on deterministic physical formulations, never express the certainty of future phenomena, but announce them within margins of error.

We have also seen that the estimate of the seismic hazard is strongly linked to the information available about past earthquakes, but with serious limitations due to the rarity of large-magnitude earthquakes, which are the ones that determine the main component of the risk. From data sets with such a small number, no significant inference can be obtained by means of statistical analyses. Not only that: given that the return times of large earthquakes generated by a seismic source (of the order of thousands of years) are typically longer than the period covered by the historical catalogs available, it can easily be assumed that the strongest earthquakes of a particular source seismic may not yet have been observed and reported in the catalogs themselves. At the same time, this can overestimate the risk of areas where a major earthquake actually occurred relatively recently.

Another typical limitation of the presently used seismic codes can be found in the full adoption of a memory-less Poisson hypothesis of the seismogenic process. It can be shown that, at least in some cases, a renewal time-dependent model can provide a better likelihood for earthquake forecasting. This alternative approach could be used in a decision-making process of optimization of the resources available for long-term earthquake risk mitigation measures.

From the above considerations, it follows the need not to limit studies for the assessment of seismic hazard to the analysis of historical and / or instrumental seismic catalogs, but to integrate them with information related to the physical and geological characteristics of the sources of earthquakes (for example, the geometric dimensions of the active faults and the average velocity of the relative sliding motion between two plates). Our conclusion is in agreement with what had been already stated by Burrato et al. [2012], in their study of the Emilia, 2012 earthquakes. Moreover, in a more recent paper Valensise et al. [2020] concluded that *“given the typical length of the seismic cycle in Italy (centuries to millennia), the mutual interaction between historical earthquake data and geological and instrumental evidence may be the only way to constrain a number of seismological issues that would be very hard to address using instrumental data alone”*.

In this respect, the application of earthquake simulators based on the physical modeling of seismogenic fault systems can constitute an additional tool contributing to a better understanding and predictability of seismogenic processes.

**Acknowledgements.** We acknowledge the contribution of all the authors of the papers quoted in this article, whose results were included as basic ingredients in several parts of our review.

We are grateful to the AE, Prof. Eleftheria Papadimitriou, and two anonymous reviewers for their encouraging comments and suggestions.

## References

- Bally, A. W., L. Burbi, C. Cooper and R. Ghelardoni (1988). Balanced sections and seismic reflection profiles across the central Apennines, Mem. Soc. Geol. It. 35, 257-310.
- Burrato, P., P. Vannoli, U. Fracassi, R. Basili and G. Valensise (2012). Is blind faulting truly invisible? Tectonic-controlled drainage evolution in the epicentral area of the May 2012, Emilia-Romagna earthquake sequence (northern Italy), Ann. Geophys., 55, 4, 2012; doi:10.4401/ag-6182.

- Console, R., D. Pantosti and G. D'Addezio (2002). Probabilistic approach to earthquake prediction, *Ann. Geophys.*, 45, 435-449.
- Console, R., M. Murru, G. Falcone and F. Catalli (2007). Stress interaction effect on the occurrence probability of characteristic earthquakes in Central Apennines, *J. Geophys. Res.*, 113, B08313, doi:10.1029/2007JB005418.
- Console, R., Murru, M., Falcone, G. and F. Catalli (2008). Stress interaction effect on the occurrence probability of characteristic earthquakes in Central Apennines, *J. Geophys. Res.*, 113, B08313, doi:10.1029/2007JB005418.
- Console, R., M. Murru and G. Falcone (2010). Perturbation of earthquake probability for interacting faults by static Coulomb stress changes, *J. Seismol.*, 14, 1 67-77.
- Console, R., P. Vannoli and R. Carluccio (2018). The Seismicity of the Central Apennines (Italy) Studied by Means of a Physics-Based Earthquake Simulator, *Geoph. J. Int.*, 212, 916-929, doi:10.1093/gji/ggx451.
- Console, R., R. Carluccio, M. Murru, E. Papadimitriou and V. Karakostas (2022). Physics-based simulation of spatiotemporal patterns of earthquakes in the Corinth Gulf fault system, *Bull. Seism. Soc. Am.*, 112, 98-117, doi:10.1785/0120210038.
- Cosentino, D., P. Cipollari, P. Marsili and D. Scrocca (2010). Geology of the central Apennines: a regional review. In: (Eds.) Beltrando M., A. Peccerillo, M. Mattei, S. Conticelli and C. Doglioni, *The Geology of Italy: tectonics and life along plate margins*, *J. Virtual Expl.*, 36, 12, doi:10.3809/jvirtex.2010.00223.
- Davies, G., J. Griffin, F. Løvholt, S. Glimsdal, C. Harbitz, H. Kie Thio, S. Lorito, R. Basili, J. Selva, E. Geist, M. A. Baptista (2018). A global probabilistic tsunami hazard assessment from earthquake sources, *Geological Society, London, Special Publications*, 456, 1, 219-244, doi:10.1144/SP456.5.
- Della Vedova, B., S. Bellani, G. Pellis and P. Squarci (2001). Deep temperatures and surface heat flow distribution. In: *Anatomy of an orogeny: the Apennines and adjacent mediterranean basins*. The Netherlands: Springer, 65-76. doi:10.1007/978-94-015-9829-3.
- DISS Working Group (2021). Database of Individual Seismogenic Sources (DISS), Version 3.3.0: A compilation of potential sources for earthquakes larger than M 5.5 in Italy and surrounding areas. <https://diss.ingv.it/>, Istituto Nazionale di Geofisica e Vulcanologia (INGV), doi:10.6092/INGV.IT-DISS3.3.0.
- Guidoboni, E., A. Comastri and G. Traina (1994). Catalogue of Ancient Earthquakes in the Mediterranean Area up to the 10<sup>th</sup> Century, ING e SGA Storia Geofisica Ambiente, Bologna, ISBN 88-85213-06-5, 504.
- Guidoboni, E. and A. Comastri (2005). Catalogue of earthquakes and tsunamis in the Mediterranean area from the 11<sup>th</sup> to the 15<sup>th</sup> century, ING e SGA Storia Geofisica Ambiente, ISBN 88-85213-10-3, 1.037.
- Hasterok, D., J. A. Halpin, A. S. Collins, M. Hand, C. Kreemer, M. G. Gard and S. Glorie (2022). New Maps of Global Geological Provinces and Tectonic Plates, *Earth-Sci. Rev.*, 231, doi:10.1016/j.earscirev.2022.104069.
- Mc Cann, W. R., S. P. Nishenko, L. R. Sykes and J. Krause (1979). Seismic gaps and plate tectonics: seismic potential for maior boundaries, *Pure Appl. Geophys.*, 117, 1082-1147.
- Meletti, C., W. Marzocchi, V. D'Amico, G. Lanzano, L. Luzi, F. Martinelli, B. Pace, A. Rovida, M. Taroni F. Visini and MPS19 Working Group (2021). The new Italian seismic hazard model (MPS19), *Ann. Geophys.*, 64, 1, doi:10.4401/ag-8579.
- Nishenko, S. P. and R. Buland (1987). A generic recurrence interval distribution for earthquake forecasting, *Bull. Seismol. Soc. Am.*, 77, 4, 1382-1399, doi:10.1785/BSSA0770041382.
- Nomikou, P., S. Carey, D. Papanikolaou, K. Croff Bell, D. Sakellariou, M. Alexandri, K. Bejelou (2012). Submarine volcanoes of the Kolumbo volcanic zone NE of Santorini Caldera, Greece, *Glob. Planet. Change*, 90-91, 135-151, doi:10.1016/j.gloplacha.2012.01.001.
- Pantosti, D. (2000). Earthquake recurrence through time, in "Proceeding of the Hokudan International Symposium and School on Active Faulting", Awaji Island, Hyogo, Japan, 17th-26th January 2000", 363-365.
- Pirazzoli, P. A., J. Thommeret, Y. Thommeret, J. Laborel and L. F. Montaggioni (1982). Crustal block movements from Holocene shorelines: Crete and Antikythira (Greece), *Tectonophysics*, 86, 27-43.
- Reid, H.F. (1910). *The Mechanics of the Earthquake, The California Earthquake of April 18, 1906*, Report of the State Investigation Commission, Vol. 2, Carnegie Institution of Washington, Washington, D.C.
- Rovida, A., M. Locati, R. Camassi, B. Lolli, P. Gasperini and A. Antonucci (2022). Catalogo Parametrico dei Terremoti Italiani (CPTI15), versione 4.0. Istituto Nazionale di Geofisica e Vulcanologia (INGV). <https://doi.org/10.13127/CPTI/CPTI15.4>.
- Rundle, J. B., S. Stein, A. Donnellan, D. L. Turcotte, W. Klein and C. Saylor (2021). The complex dynamics of earthquake fault systems: new approaches to forecasting and nowcasting of earthquakes, *Rep. Prog. Phys.* 84, 076801, doi:10.1088/1361-6633/abf893.

- Schmid, S. M., B. Fügenschuh, A. Kounov, L. Matenco, P. Nievergelt, R. Oberhansli, J. Pleuger, S. Schefer, R. Schuster, B. Tomljenovic, K. Ustaszewski, D. J.J. van Hinsbergen (2020). Tectonic units of the Alpine collision zone between Eastern Alps and western Turkey, *Gondwana Res.*, doi: 10.1016/j.gr.2019.07.005.
- Schwartz, D. P. and K. J. Coppersmith (1984). Fault behavior and characteristic earthquakes: examples from the Wasatch and San Andreas Fault Zones, *J. Geophys. Res.*, 89, 5681-5698.
- Serpelloni, E, A. Cavaliere, L. Martelli, F. Pintori, L. Anderlini, A. Borghi, D. Randazzo, S. Bruni, R. Devoti, P. Perfetti and S. Cacciaguerra (2022). Surface Velocities and Strain-Rates in the Euro-Mediterranean Region From Massive GPS Data Processing, *Front. Earth Sci.* 10:907897, doi: 10.3389/feart.2022.907897.
- Shimazaki, K and T. Nakata (1980). Time-predictable recurrence model for large earthquakes, *Geophys. Res. Lett.*, 7, 279-282.
- Stucchi, M., C. Meletti, V. Montaldo, A. Akinci, E. Faccioli, P. Gasperini, L. Malagnini and G. Valensise (2004). Pericolosità sismica di riferimento per il territorio nazionale MPS04 [Data set]. Istituto Nazionale di Geofisica e Vulcanologia (INGV), doi:10.13127/sh/mps04/ag.
- Valensise, G., G. Tarabusi, E. Guidoboni and G. Ferrari (2017). The forgotten vulnerability: a geology- and history-based approach for ranking the seismic risk of earthquake-prone communities of the Italian Apennines, *Int. J. Dis. Risk Red.*, 25, 289-300, doi:10.1016/j.ijdr.2017.09.014.
- Valensise, G., P. Vannoli, P. Burrato and U. Fracassi (2020). From Historical Seismology to seismogenic source models, 20 years on: Excerpts from the Italian experience, *Tectonophysics*, 774, 228189, doi:10.1016/j.tecto.2019.228189.
- Vannoli, P., G. Martinelli and G. Valensise (2021). The seismotectonic significance of geofluids in Italy, *Frontiers in Earth Sciences*, 9, doi: 10.3389/feart.2021.579390.
- Wesnouski, S. (1994). The Gutenberg-Richter or Characteristic Earthquake Distribution, Which Is It, *Bull. Seismol. Soc. Am.*, 84, 6, doi:10.1785/BSSA0840061940.